

Award Accounts

The Chemical Society of Japan Award for Creative Work for 2003

Electroanalytical Chemistry with Carbon Film Electrodes and Micro and Nano-Structured Carbon Film-Based Electrodes

Osamu Niwa

National Institute of Advanced Industrial Science and Technology, Central 6, 1-1-1 Higashi, Tsukuba, Ibaraki 305-8566

Received September 30, 2004; E-mail: niwa.o@aist.go.jp

The recent development of electroanalysis using carbon film electrodes and micro and nano-structured carbon film based electrodes is reviewed. Graphite-like carbon film was synthesized by various methods such as thermal chemical vapor deposition and the thermolysis of organic polymers. Highly stable diamond film electrodes with a wide potential window have been synthesized by using the plasma CVD process and then employed for electroanalysis. A carbon film consisting of electron cyclotron resonance (ECR) sputter-deposited carbon films containing a large portion of sp^3 bonds was introduced. The film makes it possible to detect analytes with higher oxidation potential or electroactive species that foul the electrode surface after oxidation. ECR carbon film can be deposited at low temperature and is conductive without doping. Graphite-like carbon films have been formed in order to construct various microelectrodes and microarray electrodes by using photolithography and dry etching methods to meet the requirements for improving the detection limit and for miniaturizing electrochemical detectors for small volume samples. For example, carbon film fabricated into an interdigitated array (IDA) electrode has a very low detection limit for biochemicals such as catecholamines when used as an electrochemical detector for high-performance liquid chromatography (HPLC) and capillary electrophoresis (CE). In contrast, composite carbon films containing various metal nanoparticles can be used for many analytes, including hydrogen peroxide and sugars. The films are deposited by the RF co-sputtering of metal and carbon. This is unlike other preparation methods such as the thermolysis of a polymer–metal complex or the electroplating of metal particles onto carbon film. The obtained carbon film contains 2–5 nm metal particles such as Pt, Ni, Cu, and Ir. The highly sensitive and extremely stable detection of hydrogen peroxide, which is known to be the product of various oxidase enzymatic reactions, was achieved with sputter-deposited carbon film in which Pt nano-particles were dispersed. In contrast, carbon films containing dispersed Ni and Cu nanoparticles provide a high electrocatalytic current for sugars such as glucose and lactose in alkaline solution. By using the film as a detection electrode for HPLC, one can obtain a lower detection limit for several sugars than when using bulk metal electrodes.

Electrochemical detection techniques are widely employed. They include the use of electrodes for voltammetry, high performance liquid chromatography (HPLC), and capillary electrophoresis (CE).[1] In addition to the continuing use of traditional instrumental analysis such as liquid chromatography, interest has been growing in the application of electroanalytical techniques to small-volume samples such as the real-time measurement of living cells. Microelectrodes have been studied theoretically and experimentally since the early 1980's.[2,3] They are of interest not only for measuring local areas, but also for several other reasons, including small iR drop, the fast establishment of a steady state current, and a small capacitive current. Traditionally, microelectrodes have been fabricated from metal wires and carbon films into microdisk, microring and microcylinder shapes. The size of such electrodes is typically 1 to 10 μm; they are employed for the in vivo and in vitro monitoring of biochemicals such as neurotransmitter release.[4,5] Wightman et al. used carbon fiber electrodes with diameters of 1 to a few μm for detecting catecholamines secretion by exocytosis.[4,6] They modified the carbon fiber electrode with an anionic polymer such as Nafion and overoxidized polypyrroles to reject L-ascorbic acid and 3,4-dihydroxyphenylacetic acid (DOPAC), which is the metabolite of dopamine. However, the microelectrode techniques have certain limitations as regards, for example, the imaging of biochemicals or mutli-analyte detection. Microelectrodes fabricated from metal films such as gold and Pt were reported in the mid 1980's. Wrighton et al. reported an electrochemical field-effect transistor using closely spaced microelectrodes modified with a conducting polymer such as polypyrrole.[7] The current flow between two microelectrodes can be controlled by changing the polymer doping level by changing the potential. Bard et al. reported the voltammetry of redox species using two or three closely spaced microband electrodes.[8] At the same time, our group produced microband array and microdisk array electrodes by using a microfabrication technique where we deposited silicon oxide insulating film on an indium tin oxide (ITO) film electrode. We employed these electrodes to form conducting poly-

Published on the web April 8, 2005; DOI 10.1246/bcsj.78.555

mer patterns with polymers such as polypyrrole in an insulating polymer by electrochemical polymerization.[9] Microfabricated electrodes became more widely used in electrochemistry after the late 1980's. Electrodes with various designs including microband, microdisk array and interdigitated array (IDA) electrodes were fabricated for use in voltammetry and flow analysis.[8,10,11] Microfabricated electrodes have much better electrochemical performance characteristics than traditional microelectrodes and macro-size electrodes. However, until the early 1990's, almost all lithographically fabricated microelectrodes were made from metal films such as gold and Pt. However, the fact that metal film electrodes have narrower potential windows and higher background currents than carbon electrodes limits the analyte that can be measured and reduces the detection limit. Therefore, the fabrication of carbon films with good electrochemical properties started to become very important. Carbon films for electroanalysis have been fabricated by various methods, including the pyrolysis of gases,[12] the pyrolysis of sublimed organic films,[13–15] carbon film sputtering,[16,17] the pyrolysis of photoresists,[18] the pyrolysis of conducting polymer films,[19] and the patterning of organic films such as polyacrylnitrile.[20] More recently, various kinds of new carbon films have been reported. Boron-doped diamond electrode film prepared by plasma chemical vapor deposition (CVD) has an extremely wide potential window and is chemically stable. Therefore, it can detect analytes with a high oxidation potential such as histamine and chlorophenols.[21–23] McCreery et al. reported carbon films with extremely flat surfaces prepared on highly doped silicon by electron beam evaporation.[24] In contrast, our group prepared carbon film consisting of sp^2 and sp^3 bonds and with an extremely flat surface by the electron spin cyclotron (ECR) sputtering method.[25]

To realize a carbon film based microelectrode with a practical fabrication process, we first fabricated a carbon based IDA electrode from graphite-like carbon film by using photolithography and reactive ion etching (RIE). This carbon-based IDA provides excellent electrochemical characteristics, including higher sensitivity, a wider potential window, and a lower background current than those of metal film-based IDA electrodes.[14,15] Since carbon film is suitable for achieving a low detection limit, we fabricated carbon film-based microdisk array, ring-disk, split disk, and micro-ring electrodes[26] and employed them as electrochemical detectors for LC and CE.[27] Microfabricated film electrodes have become more important since the recent development of miniaturized sensors and the micro total analytical system (μ-TAS) requires miniaturized electrochemical detectors that are realized by fabricating the film in the microfluidic device. Mathies et al. reported the integration of metal film-based electrochemical cells in a microflow channel for capillary electrophoresis. They achieved the separation and detection of catecholamines in nano-liter volume samples.[28] Baldwin et al. also reported film electrodes as fully integrated detection electrodes for on chip capillary electrophoresis.[29] As mentioned above, carbon film is more suitable for such purposes. Carbon film-based electrodes modified with enzymes on the glass chip were incorporated in the flow channel.[30] These carbon film-based microbiosensors can be used with low concentrations of biochemicals and low sample volumes as in the real-time measurement of in vivo and in vitro neurotransmitters and metabolites.[31,32]

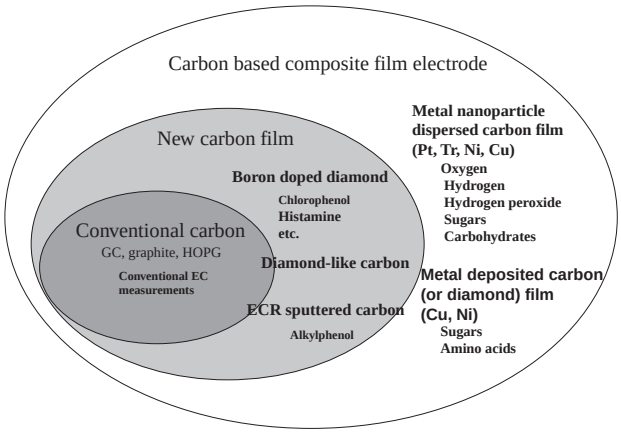

Fig. 1. Detectable analytes by pure and composite carbon films.

Although carbon film based electrodes exhibit excellent electrochemical characteristics, such as a wider potential window than metals and a low background noise level, they can only detect a limited number of analytes. This is because some analytes have a high over-potential at the carbon electrodes. For example, hydrogen peroxide, which is the product of various oxidase enzymes such as glucose, L-glutamate and lactate, is usually detected with electrodes made of metals such as platinum (Pt) or palladium (Pd) at around 500 mV (vs Ag/AgCl). However, the detection potential with carbon electrodes is higher than that with a metal electrode by about 200 mV. Figure 1 shows the analytes that can be detected by the various carbon-based electrodes. Although new carbon films such as boron-doped diamond, diamond-like carbon and ECR sputter-deposited carbon films can detect analytes with higher oxidation potential, it is preferable to use electrodes that contain metal for measuring hydrogen peroxide, sugars, and amino acids. It is well known that Pt, iridium (Ir), and Pd electrodes are suitable for measuring hydrogen peroxide, which is the product of oxidase enzymes. It is also known that carbohydrates and amino acids can be detected in alkaline media with the constant potential application method using electrodes made of transition metal such as copper (Cu) and nickel (Ni).[33] However, pure metal electrodes are not suitable for highly sensitive detection due to their high background current and unstable surface. A composite electrode made of carbon and metal is a sophisticated solution. Since each metal nanoparticle in (or on) the carbon film works as a nanoelectrode, very high sensitivity can be expected with composite electrodes. Several methods have been reported for preparing metal clusters on carbon film, including the vapor or electro-deposition of metals directly onto the electrode surface and the entrapment of metals within a polymer film affixed to the electrode.[34] Electrochemical deposition has been most commonly used to prepare metal clusters such as Pt and Pd clusters on the carbon electrode surface and is mainly employed for studying fuel cell electrodes. However, several groups have prepared metal deposited carbon electrodes including GC and boron-doped diamond film electrodes for electroanalysis. Cu/Cu oxide or Cu oxyhydroxide modified GC, cobalt oxyhydroxide film dispersed carbon,[35] and Ni and Cu modified GC[36] or dia-

mond film[37] have been used to measure amino acids, carbohydrates and alditol, nitrous oxide and carbohydrates, respectively. Most of the above methods can produce nanoparticles on an electrode surface. However, very few papers have reported the preparation of uniform Pt-cluster dispersed carbon film. Composite-type carbon film electrodes have also been prepared by various methods such as the pyrolysis of polymer film and metal complexes.[38] In contrast, our group prepared composite carbon films by the RF co-sputtering of metal and carbon.[39] When metal nanoparticles are dispersed in carbon film, high electrocatalytic activity can be expected. However, such a nano-structure cannot be fabricated even with current nanolithography. The phase separation of metal and carbon realizes metal nanoarray electrodes in the carbon film.

This paper introduces the preparation and electrochemical properties of new carbon films and focuses particularly on our ECR-sputter deposited carbon film. This work then reviews the electrochemical properties of these microfabricated carbon films and their applications to the measurement of biochemicals. Finally, carbon film electrodes containing dispersed metal nano-particles and prepared by the RF sputtering method are described.

1. Electron Cyclotron Resonance (ECR) Sputtered Carbon Film Electrodes for Electrochemical Measurements

As mentioned in the introduction, carbon films have been fabricated by various procedures. Most carbon films have a graphite-like structure; thus the film consists of sp^2 carbon bonds. Figure 2A shows the Raman spectra of carbon films prepared by the thermolysis of organic film. This carbon film has two broad peaks at 1590 and 1340 cm^{-1}, indicating that the film is similar to glassy carbon. The interpolate spacing is 0.36 nm, which is a little larger than that of crystal graphite, showing the structure is slightly disordered graphite.[15] The film has a much wider potential window and lower background current than Pt or gold based film electrodes, as shown by the voltammograms in Fig. 2B.

More recently, new carbon film electrodes have been employed for electroanalytical chemistry. The boron-doped diamond film electrode, which is usually obtained in polycrystalline form by plasma CVD at around 700 °C, consists of sp^3 bonds, and is thus highly stable with respect to extremely high anodic oxidation and chemically extremely aggressive media.[21–23] Many electrochemists have employed diamond film electrodes for measuring polyamines, azide anions, chlorophenols, L-cysteine, and histamine, due to the relatively low signal to background current ratio, wide potential window and mechanical robustness of diamond film.[40,41] In contrast, diamond-like carbon (DLC) film has been prepared by the CVD process, sputtering,[42] or ion source techniques. The electrochemical properties of this film, such as the width of the potential window, were limited by the sp^2 bonds in the film. Zeng et al. reported nitrogen-doped diamond-like carbon film that they deposited on a silicon wafer with a DC magnetron sputtering system.[43] The reported film has a low double layer capacitance, a large electrochemical potential window, and a relatively high electrochemical activity as regards ferricyanide reduction. Hirono et al. reported a new carbon film fabricated by ECR plasma sputtering, whose hardness is comparable to that

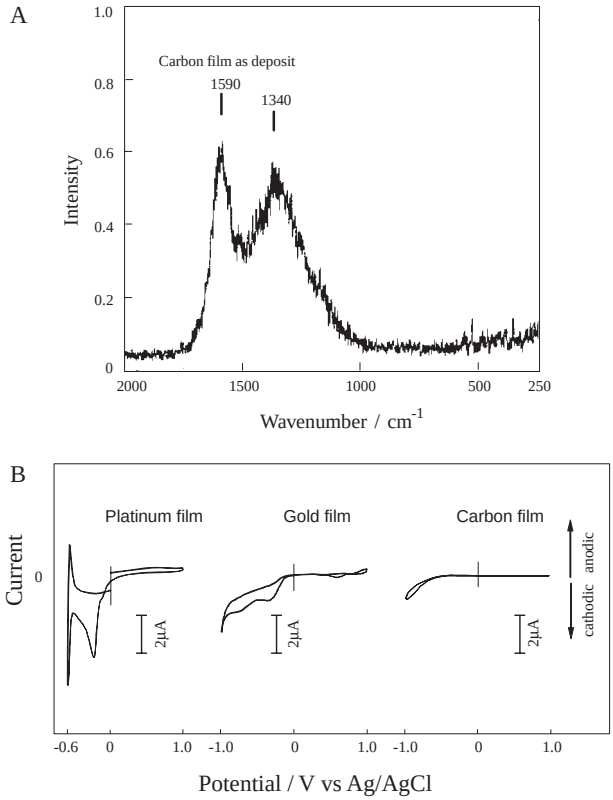

Fig. 2. (A) Raman spectra of the carbon films by pyrolysis of poly-perilene film deposited on surface oxidized silicon wafer by thermal chemical vapor deposition. (B) Voltammograms at the Pt, gold and carbon film electrodes in pH 7 phosphate buffer (0.1 M).[15]

of diamond but whose conductivity is 19 orders of magnitude larger.[44] Unlike previously reported graphite-like carbon film, ECR sputter-deposited carbon film is deposited on silicon substrates and consists mainly of sp^2 nanocrystallite carbon with parallel and curved graphite sheets vertically oriented to the film surface. The sp^2 nanocrystallites are connected with adjacent crystallites by sp^3 bonds, which gives the film both its diamond-like hardness and its high conductivity. With the ECR sputtering method, the sp^3 bond content can be controlled by controlling the ion irradiation of the growing surface during deposition.[45] We characterized the film with a view to employing it as an electrode for voltammetry and flow injection analysis. A mean roughness (Ra) of 6.9×10^{-2}, and a roughness profiles of between 1.65 and 2.05 nm were confirmed by AFM images of a 500×500 nm^2 area. This means that the ECR sputter-deposited carbon film is very smooth (the surface roughness variation is only about $+/-$ 0.2 nm).[25] The surface is much flatter than that of poly-crystalline diamond and comparable to that of the pyrolyzed amorphous carbon film prepared by electron beam evaporation reported by McCreery et al.[24] Figure 3 shows high-resolution XPS spectra and the decomposition of the C_{1s} of the ECR-sputtered carbon film. The C_{1s} XPS spectra can be decomposed into 6 peaks (C1–C6); C1 (284.3 eV) and C2 (285.3 eV) are assigned to the sp^2 (C=C) and sp^3 (C–C) bonds, respectively, which is almost the same assignment that reported by Diaz et al.[44] The sp^3/sp^2

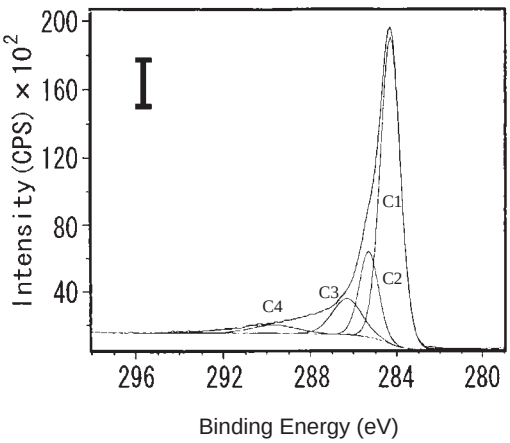

Fig. 3. XPS spectra of ECR sputter deposited carbon film of high resolution decomposition of C_{1s} XPS peak.[25]

ratio for ECR sputtered carbon film is 27.4%. The sp^2 bonded carbon is the main region of the carbon film, but there is also a small sp^3 region in the film that forms a cubic lattice connecting different sp^2 rings. The $sp^3/(sp^2 + sp^3)$ ratio can be increased up to 85.0% and the shoulder peak assigned to the sp^3 bond then becomes clearer.[45] The harder film with the higher sp^3 content is as hard as diamond film. The C3 and C4 peaks are assigned to the C–O bond caused by oxygen on the film surface. The conductivity of the ECR-sputtered carbon film is different from that of GC film. The conductivity of ECR carbon film is 35 S/cm, while the value is 100–1000 S/cm for GC film.[45] The higher conductivity of the GC film may be because its crystalline structure is larger than that in the ECR carbon film. However, the relatively high conductivity of ECR carbon film compared with that of conventional amorphous carbon (usually $\sim 10^{-2}$ S/cm)[46] suggests that the structure is not completely amorphous and might be nanocrystalline, which is difficult to observe by AFM. The D and G Raman peaks of ECR carbon are broader than those of HOPG and GC. This also supports the idea that the structure of ECR carbon film is different from that of diamond, HOPG and GC film.

ECR carbon film has some interesting electrochemical properties. First, the potential window of the film is wider than that of GC, which makes it possible to measure analytes with higher oxidation potential. The ECR film can be used for measuring alkylphenols, which are a biodegradation product of commonly used alkylphenol ethoxylate (APEs). Alkylphenols, especially ρ-nonylphenol, are toxic; they are known to be endocrine disruptors.[47] It is easy to electrochemically oxidize alkylphenols at carbon electrodes. However, the surfaces of GC and graphite-like carbon electrodes are easily passivated and the electrochemical response quickly becomes smaller. Consecutive cyclic voltammetry measurements for ECR carbon, GC and graphite carbon films show that the peak oxidation current of ρ-nonylphenol decreases cycle by cycle at each carbon electrode. However, the magnitude of the anodic peak current after 5 consecutive cycles is much greater than the magnitudes obtained with GC and graphite-like carbon.[25] Moreover, the oxidation current of ρ-nonylphenol at an ECR carbon film electrode can be restored to its original value after a 5 min interval between cycles without the need for stirring or any pretreatment of the film electrode. Figure 4A shows the changes in the peak currents for five kind of alkylphenols: (ρ-pentylphenol, PP; ρ-hexylphenol, HP; ρ-heptylphenol, TP; ρ-octylphenol, OP; ρ-nonylphenol, NP) at the ECR carbon, GC and graphite-like film electrodes as a function of time. The peak currents of alkylphenols with longer alkyl-chains initially exhibit higher peaks since they can be pre-concentrated on the electrode surface due to their hydrophobicity. However, these peak currents decrease very rapidly at GC and graphite-like carbon film. In contrast, the peak currents change very little during the long measurement period with ECR carbon film, indicating that the surface of an ECR carbon film electrode is less easily passivated by the oxidized products of alkylphenols than the other carbon electrodes. Figure 4B shows the effects of electrochemical pretreatment on the detection of the same alkylphenols at ECR carbon films. Compared with the current changes seen in Fig. 4A, the peak currents of the alkylphenols decrease rapidly at the pretreated ECR carbon film electrodes. There are two possible reasons for the changes in the current response. One is that the surface structure changed after electrochemical pretreatment, which increased the density of the oxygen-containing groups at the ECR carbon film. XPS measurements undertaken before and after electrochemical pretreatment show that the ratio of O/C for the ECR carbon film surface increases from 5.3% to 45.0%. A lower concentration of oxygen-containing groups in the unpretreated ECR carbon film results in less adsorption of alkylphenols. The other possible reason relates to the flat surface of the ECR carbon film, since it allows the electrochemically oxidized products of alkylphenols adsorbed on the ECR carbon film to be removed more easily than from other carbon-based electrodes. The sub-nanometer order flat surface of the ECR carbon film is better in terms of micro- or nano-fabrication than diamond film. The microfabrication of ECR carbon film is now being developed for application to electrochemical detectors for LC, CE and various sensors and micro-analytical devices. However, the film is still being studied, since a higher potential window and less adsorptive properties could be achieved if a film with a higher sp^3 content can be developed with in-situ doping to increase conductivity.

2. Micro- and Nano-Fabricated Carbon Films Produced with Lithographic Technology

2.1 Microfabrication of Carbon Film. Various microelectrodes and microarray electrodes have been fabricated from carbon films. We have reported electrochemical measurements that we undertook using various carbon film-based microarray electrodes. It is more complicated to microfabricate carbon film than metal films. Figure 5 shows a schematic representation of the microfabrication procedures for carbon films compared with those for metal films. With metal films, the etching or lift-off methods are usually used, as shown in Figs. 5(a) and (b). To etch the metal film, the electrode pattern is covered with a photoresist polymer pattern fabricated using photolithography. Then, the metal film not covered by the resist film is removed by wet etching or ion milling methods. However, with carbon film, the resist film etches faster than the carbon film when oxygen plasma is applied. With the

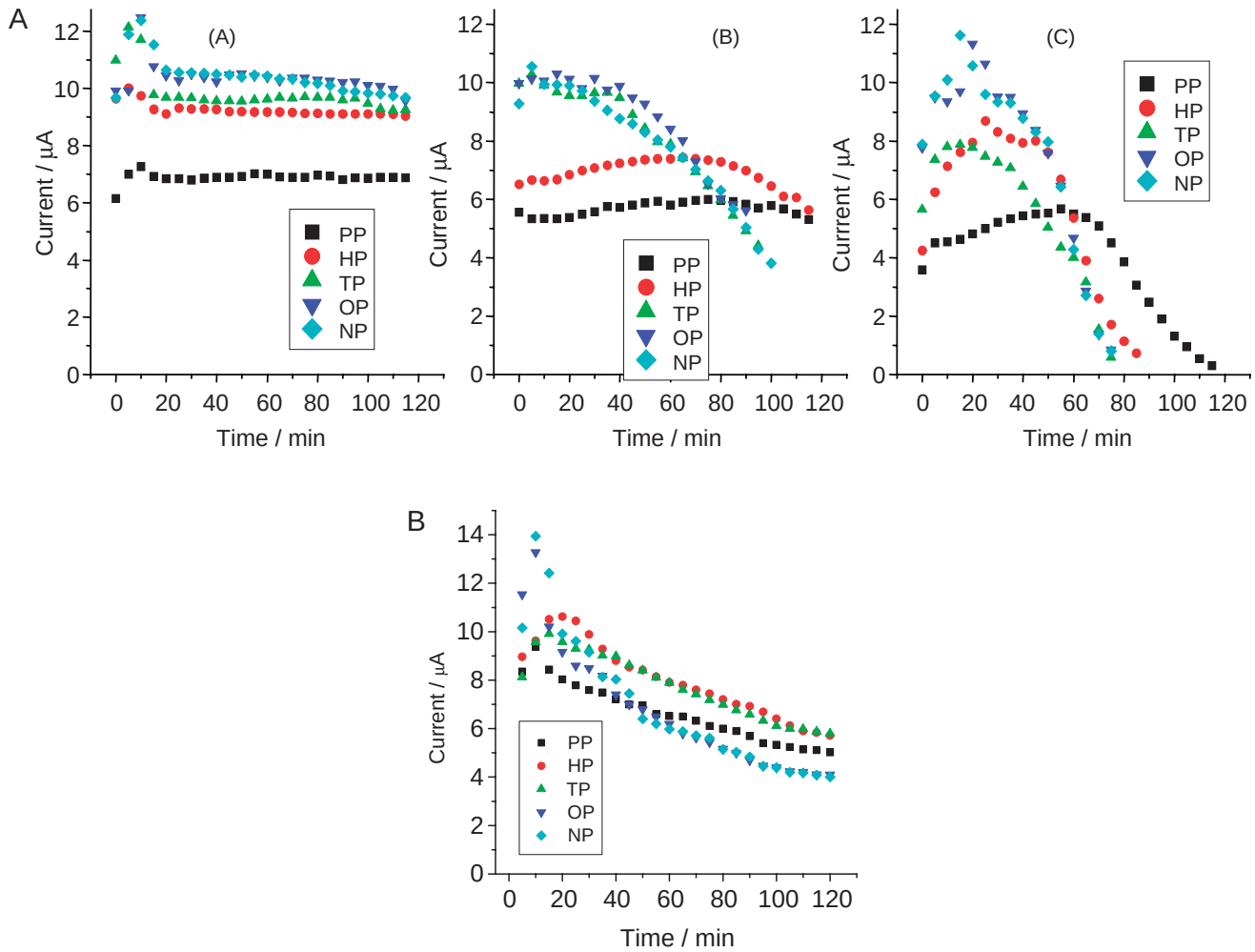

Fig. 4. (A) Variation in the anodic peak current of CVs for 100 μM alkylphenols (PP, TP, HP, OP, NP) obtained at (a) ECR carbon film, (b) GC and (c) graphite-like carbon electrodes (d. = 3 mm) without pretreatment. The interval between each measurement is 5 min. 0.1 M phosphate buffer solution, pH 7; Potential scan rate is 100 mV/s.[25] (B) Effect of electrochemical pretreatment on anodic peak current of CVs for alkylphenols at the ECR carbon film electrode. The electrode was electrochemically pretreated in 0.1 M H_2SO_4 at 1.8 V (vs Ag/AgCl).[25]

lift-off method (Fig. 5(b)), the negative image of the desired electrode pattern is formed with photoresist by photolithography and metal film is deposited. After deposition, the electrode pattern is formed by removing the metalized resist film sonicating the metalized resist film in the solvent. However, when carbon film is deposited on the patterned photoresist to employ the lift-off process, the resist pattern is destroyed during carbon film deposition, since the deposition temperature is usually high. Therefore, the metal pattern is formed on the carbon film and the carbon electrode pattern is fabricated by etching the carbon film using the metal pattern as a mask (Fig. 5(c)).[17] We proposed a new method for obtaining a carbon film-based microelectrode, as shown in Fig. 5(d).[14,15] With our method, a polysiloxane based positive photoresist[48] is patterned on the carbon film by photolithography and the microelectrode is fabricated by etching the carbon film with oxygen plasma, using the resist pattern as a mask. The polysiloxane-based photoresist exhibits a very low etching rate with oxygen plasma because the surface of the resist turns into SiO_2 when oxygen plasma is applied. Carbon film-based microarray electrodes can be fabricated with our new process, which is similar to the process used for metal film-based microelectrodes. More recently, a photoresist-derived carbon film based microsystem was reported.[49] This method makes it possible to fabricate a microelectrode without an etching process, since the electrode is microfabricated before the patterned resist is pyrolyzed. Microdisk array electrodes can be fabricated by directly forming the insulating film patterns on the carbon film without etching the carbon layer. We pyrolyzed spin coated poly-phenylene vinylene precursor and obtained carbon film, and then fabricated microdisk array electrodes by patterning with resist coated on the carbon layer.[19] More recently, a microdisk array electrode based on boron-doped diamond film was fabricated on a structured silicon substrate.[50] With polycrystalline diamond film, a polishing process is used since the macroscopic surface is not flat.

2.2 Electrochemical Performance of Carbon Based Microelectrode Array Electrodes. Table 1 summarizes previously reported carbon film based micro and microarray electrodes and their applications. IDA electrodes are of interest be-

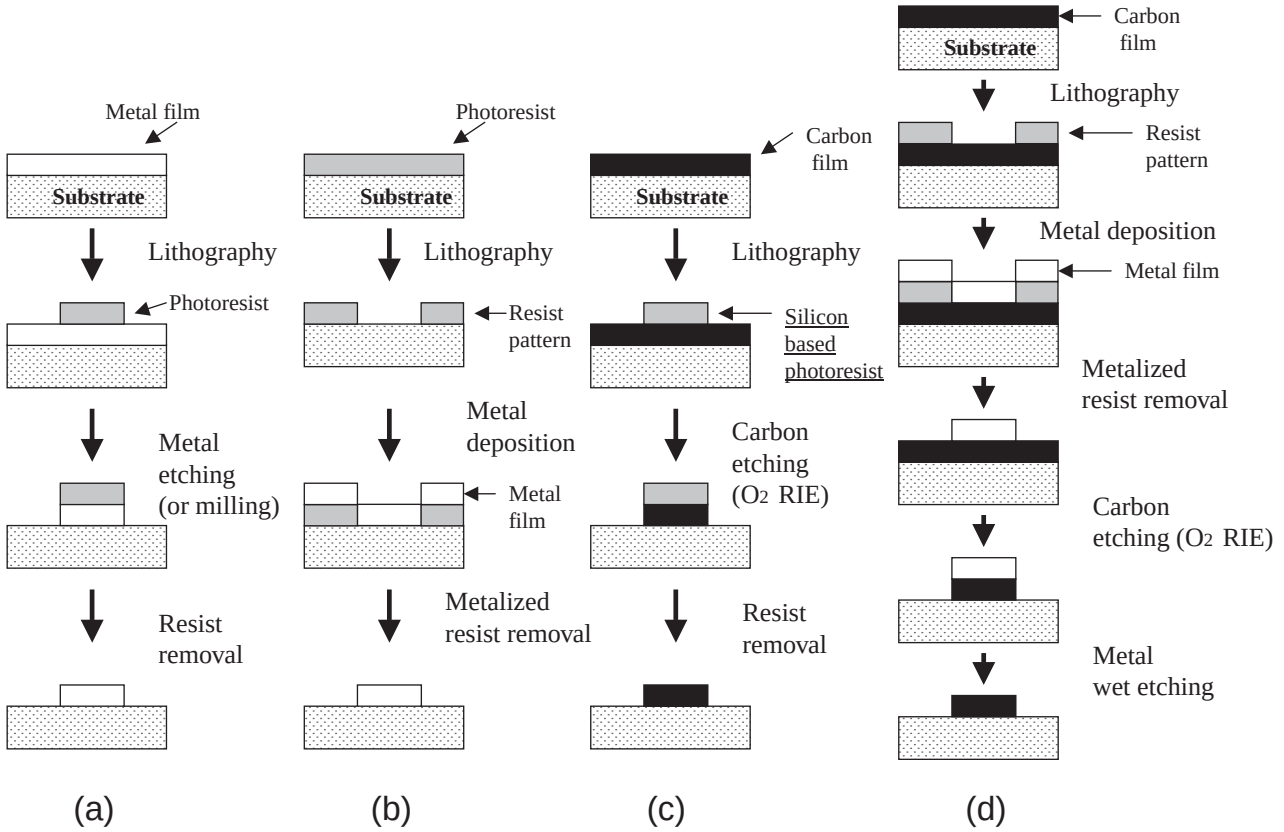

Fig. 5. Illustration of fabrication processes of metal and carbon films (a) Etching process of metal film (b) Lift-off process of metal film electrode fabrication (c) Etching process of the carbon film using metal film mask (d) Etching process of the carbon film using silicon based positive photoresist mask.

Table 1. Microfabricated Carbon Film Electrodes for Electroanalytical Chemistry

Electrode structure	Fabrication process	Measurement technique/Analyte	References
Microband	Carbonization of deposited polyacrylonitrile	Voltammetric characterization of electrode	20b
Microdisk array	Pyrolysis of conducting polymer and resist patterning on film	Voltammetry of ferrocene derivatives	19a
Microdisk array	Plasma CVD boron doped diamond film on structured Si wafer	Voltammetry of ascorbic acid and 3,4-dihydrophenyl acetic acid	50
Interdigitated array (IDA) or ring shaped IDA electrodes	Thermal CVD graphite like carbon and RIE with silicon based resist mask	Voltammetry of redox species and LC and CE of catecholamines Integrated in microfluidics	15, 26b, d, 31a, 52
IDA electrode	RF Sputter deposited carbon and RIE with metal film mask	Voltammetry of dopamine and acetaminophen	17
Microband and IDA electrode	Resist patterning and thermolysis	Voltammetric characterization of electrode	49
Ring-disk and split-disk electrodes	Thermal CVD graphite like carbon and RIE with silicon based resist mask	Generation-collection measurement and hydrodynamic voltammetry at fixed potential	26a, c
Individually addressable array electrode	Thermal CVD graphite like carbon and RIE with silicon based resist mask	Imaging of L-glutamate with enzyme modified 64 channel microarray electrodes	54b

cause of their high sensitivity and low detection limits.[10] With an IDA, the electroactive species, that is, the species generated at one band array electrode, is collected at an adjacent band array electrode when the potential is set at a level at which a reverse electrochemical reaction can take place. Therefore, the signal increases with decreasing bandwidth and IDA gap (Fig. 6A). This current enhancement by redox cycling and the lower background of the carbon films greatly improve the high signal-to-noise ratio and thus achieve a low detection limit. Figure 6B shows an SEM image of a carbon film based

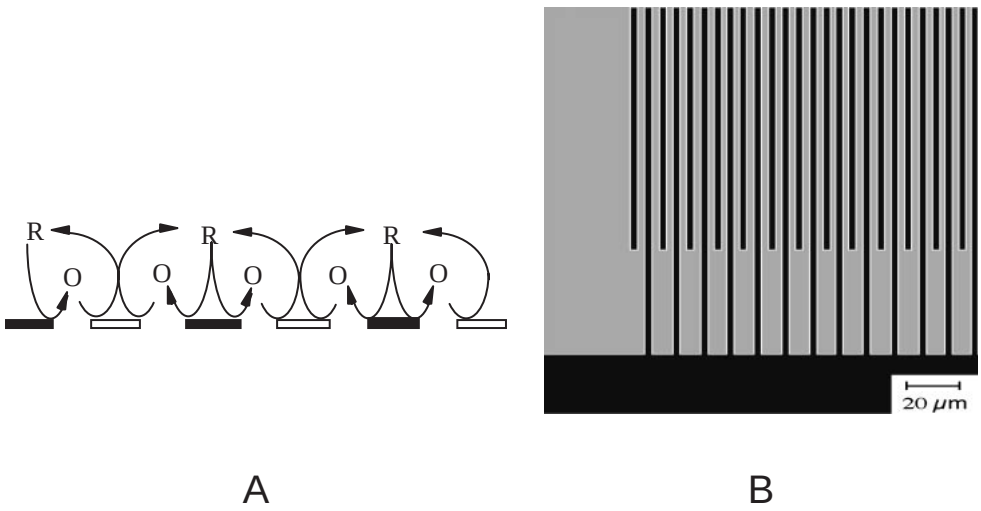

Fig. 6. Schematic representation of redox cycling at the IDA (A). SEM image of carbon film based IDA electrode (B).

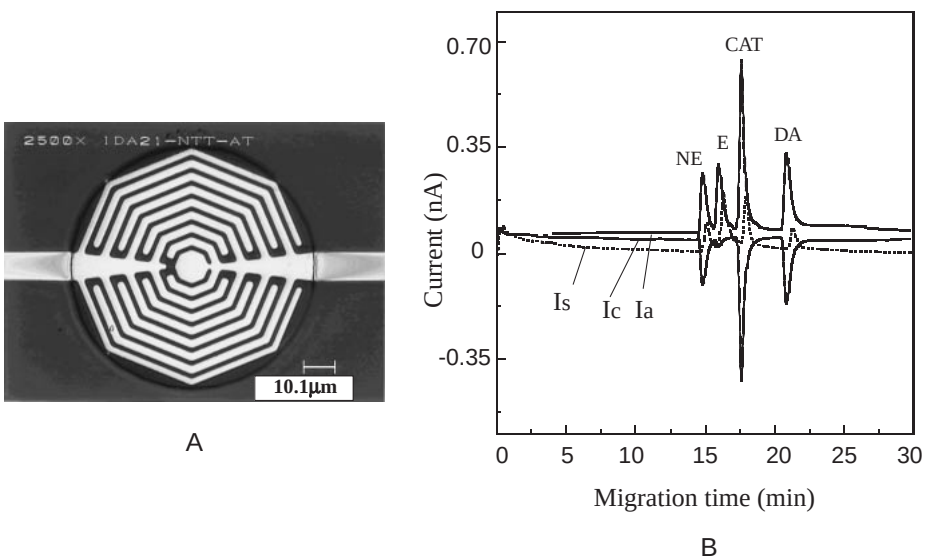

Fig. 7. SEM image of carbon film based ring shape IDA electrode for CE (A). Electropherograms of catecholamines obtained by capillary electrophoresis with carbon film based ring shaped IDA electrode (B). Ia and Ic are anodic and cathodic current in the dual mode, respectively. Is is anodic current in the single mode. Conditions: 65 cm × 25 μm i.d. fused silica capillary, capillary to electrode distance: 60 μm, 10 mM phosphate, 15 mM borate and 10 mM SDS as running buffer and 1 M NaOH added to obtain pH 7.0; separation parameters, 10 kV, 2.59 μA; electrokinetic sampling, 20 kV, 5 s; 20 μM NE, CAT, DA and 50 μM E; detection potentials, 700 mV on anode and −300 mV on cathode.

IDA electrode with a 2 μm bandwidth and gap.[15] In our early experiment, we achieved a low detection limit for dopamine (DA) and its metabolite: 3,4-dihydroxyphenylacetic acid (DOPAC) using a carbon based IDA electrode combined with LC. We estimated a low detection limit of 32 amoles for DA by performing a calculation with peak height and background noise level (0.1 pA) when using a Sepstik microbore C18 reversed-phase column (150 × 1 mm^2 i.d., 5 μm particle size).[27a] The detection limit was about two orders of magnitude lower than that of a commercially available glassy carbon electrode.

The electrochemical measurement technique is becoming more widely used for very low volume analyses of less than a nanoliter. For such applications, CE with electrochemical detection and on-chip electrochemical measurement have been studied. Ring-shaped carbon film IDA electrodes were developed for use as detection electrodes in the thin layer radial flow cells for LC and CE.[26,27] For CE, the detection electrode was miniaturized to a total diameter of 80 μm, which is similar to the inner diameter of the capillary. Figure 7 shows an electropherogram of catecholamine measured at carbon film based ring shaped IDA electrodes in dual and single modes. The anodic currents of these catecholamines in the dual mode (anode = 700 mV vs Ag/AgCl, cathode = −300 mV vs Ag/AgCl) were enhanced to different extents, compared with those in the single mode. The current enhancement caused by redox cycles at the ring-shaped IDA reflects its electrochemical reversibility. Therefore, the order is CAT > DA > NE > E. The current enhancement also depends on the separation volt-

Table 2. Catecholamine Detection Limits[a] at the IDRA Microelectrode in Capillary Electrophoresis

Compound	NE	E	CAT	DA
Anode in dual mode	1.1 (80 nM)	3.0 (0.23 μM)	0.42 (35 nM)	0.80 (81 nM)
Cathode in dual mode	1.8 (0.13 μM)	38 (2.9 μM)	0.50 (43 nM)	0.93 (94 nM)
Anode in single mode	3.1 (0.23 μM)	3.6 (0.28 μM)	1.5 (0.13 μM)	2.8 (0.28 μM)

a) The detection limits were obtained at S/N = 3 and the noise was 0.63 pA. The units are femtomoles. The conditions are the same as those in Fig. 5.

age. A lower voltage decreases the flow rate, which does not interfere with the redox cycling at the electrodes. The detection limits of NE, E, CAT, and DA are listed in Table 2. The detection limits of NE, E, CAT, and DA at the anode in the dual mode are much lower than those in the single mode. But the detection of E does not deteriorate significantly as a result of poor electrochemical reversibility. The concentration detection limit of CAT is lower than a published result,[51] since the electrode geometry can be designed to obtain a low detection limit with carbon film electrodes. The carbon based IDA was integrated in glass based microfluidic devices for the continuous measurement of blood catecholamines. The lowest detection limit of (110 +/− 10 pM (S/N = 3)) for reported catecholamine sensors is obtained with a low flow rate of 2 μL/min.[52] In this case, the total volume needed for measurement can be greatly reduced, since all the components, such as a micro-reactor, can be integrated with little increase in the volume.

Another advantage of the carbon film-based microarray electrodes is that they offer multi-potential or multi-analyte detection. The carbon film was fabricated into an eight-sector array (split disk) electrode for use as a low flow rate amperometric detector (Fig. 8A). This pie-shaped electrode array was combined with a thin layer flow cell, and a conversion efficiency of 94% was achieved at a flow rate of 0.01 μL/min. A coulometric hydrodynamic voltammogram of a reversible redox species was obtained by applying different potentials to each electrode in 26 mV steps with a small injection volume (5 μL/min). Figure 8B shows the hydrodynamic voltammograms obtained with the split disk electrode for 31.6 μM ferrocyanide. The electrode potentials were set circularly from 0.195 to 0.377 V in 26 mV steps. When the center of the array electrode was well aligned, no electrochemical crosstalk was observed and the current obtained at each electrode fitted well with the theoretical curve.[26c]

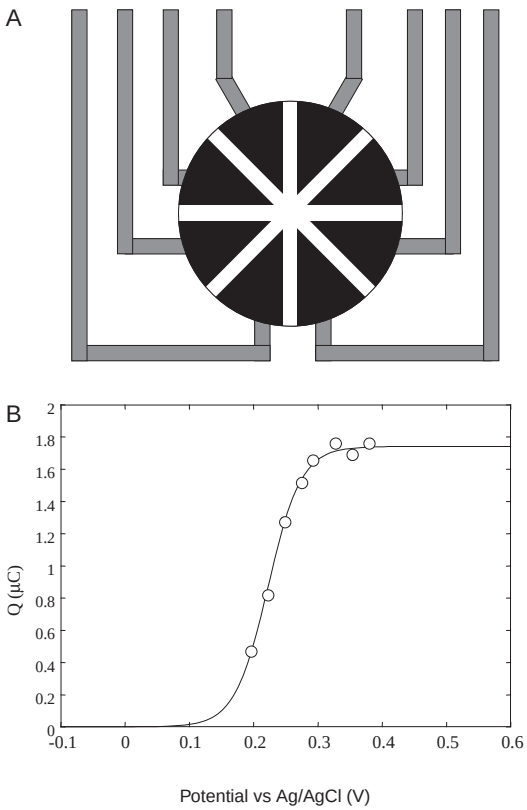

Fig. 8. Pattern of carbon film based split disk arrays consisting of 8 electrodes (A). Hydrodynamic voltammogram of ferrocyanide (31.6 μM, 5 μL, 1.9 μC) on the split disk electrode (B). The flow rate was 0.03 mL/min. Electrode potentials were set circularly from 0.195 to 0.377 V in 26 mV steps for eight electrodes. The curve were drawn according to the equation in Ref. 26(c).

Many groups used a scanning electrochemical microscope (SECM) with microelectrodes to image the electrochemical reaction.[53] This technique has been used to obtain both topological images and images of some molecules around the cells. However, an SECM image is not a real-time image, since we need to scan the electrode probe. Instead of SECM, a microelectrode array can be used for imaging the biomolecules.[54] Carbon film based microarray electrodes are important in that they enable us to detect low concentrations of analytes such as neurotransmitters. We fabricated 8 × 8 microarray electrodes (each 30 μm square) modified with Os–polyvinylpyridine based polymer (Os-gel) containing horseradish peroxidase (HRP) and glutamate oxidase (GluOx). Hydrogen peroxide generated by the enzymatic reaction of L-glutamic acid was reduced by HRP, which is also reduced electrochemically by Os-gel. A detection limit of 1 μM was achieved and the variation in glutamate concentration distribution was imaged in real time. This individually addressable microarray can be used to detect the distribution of one analyte,[54b,55] but can also be used to improve the selectivity and detection limit with a differential signal using two microelectrodes.[56] We fabricated two carbon film based dual electrodes arranged in parallel in a microfluidic channel. Figure 9 shows the response of 1 μM L-glutamate at (a) one of the electrodes in the dual mode microelectrode modified with BSA-GluOx/Os-gel-HRP bilayer films and (b) the other electrode modified with BAS/Os-gel-HRP. The cathodic current at one film electrode started to increase 10 s after glutamate injection and the current quickly reached a steady state (Fig. 9(a)), In contrast, no current increase was observed at the other electrode, which was modi-

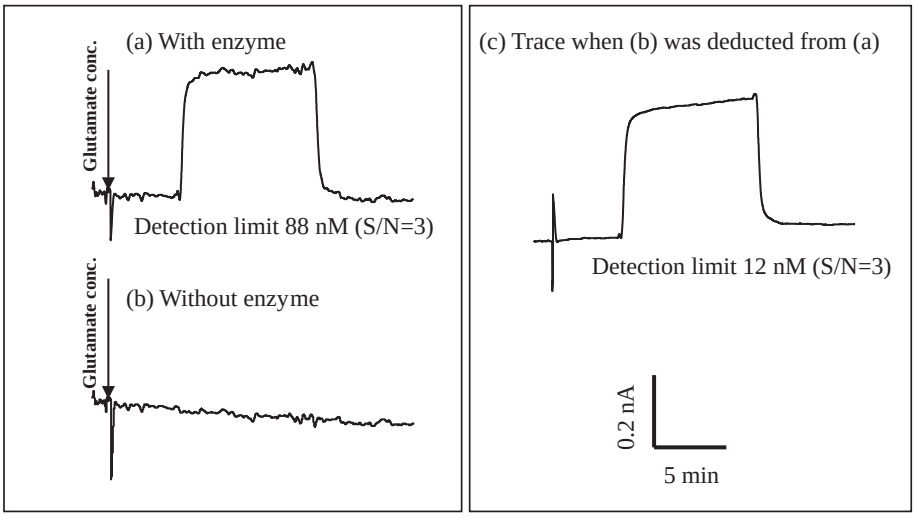

Fig. 9. The response of 1 μM glutamate with the dual microfabricated glutamate sensor. One film electrode is modified with a bilayer of BSA-GluOx/Os-gel-HRP (a), and the other electrode with a bilayer of BSA/Os-gel-HRP (b). (c) The trace obtained by deducting the current shown in (b) from that shown in (a).[56a]

fied with BSA/Os-gel-HRP without GluOx. Figure 9(c) shows a trace obtained by subtracting the current shown in (b) from that shown in (a). This result clearly shows that the electrostatic noise and pumping noise were greatly reduced, enabling us to observe just the glutamate concentration change in real time. A detection limit of 88 nM ($S/N = 3$) was calculated from trace (a). However, a lower detection limit of 12 nM ($S/N = 3$) was obtained from trace (c) because of the noise reduction realized by using the responses at the dual electrode. With this technique, we observed the variation in the glutamate concentration from cultured rat cortex neurons stimulated by KCl and we also used it to measure the histamine release from cultured rat basophilic leukemia cells (RBL-2H3) stimulated by antigen.[56]

As described in this section, carbon film based micro and microarray electrodes have many advantages over both metal film based electrodes and traditional fiber type electrodes as regards sensitivity, detection limit and selectivity. They make it possible to image biochemicals and to realize multi-analyte detection.

3. Carbon Film Electrodes Containing Dispersed Metal Nano-Particles

3.1 Preparation of Metal and Carbon Composite Film Electrodes. As described in the introduction, metal electrodes have various electrocatalytic abilities; these properties make it possible to detect more analytes than carbon based electrodes in spite of a large background noise level and a narrower potential window. Therefore, a combination of metal particles deposited on (or dispersed in) the carbon film enables us to realize metal nanoarray electrodes. Traditionally, the metal particles are deposited electrochemically onto bulk carbon electrodes. More recently, metal deposited or metal dispersed carbon films have been reported and some have been used for electroanalysis. Table 3 summarizes metal-deposited or metal nanoparticle-dispersed carbon film electrodes including boron-doped diamond film. McCreery and co-workers[38,57] have published a series of articles on the synthesis of nanoscale Pt(0) clusters in glassy carbon (not solely on a glassy carbon surface) by incorporating Pt in a glassy carbon precursor, followed by thermolysis at 600 °C. The obtained film contains 2–3 nm Pt nanoparticles. This kind of Pt(0)-doped glassy carbon (Pt–GC) exhibits high catalytic activity for the reduction of H^+ and dioxygen. Joo et al.[58] synthesized a high dispersion of Pt nanoparticles supported on ordered nano-porous arrays of carbon. Fujishima et al. reported electrochemically deposited Cu- or Ni-modified boron doped diamond films for electrocatalytically oxidizing sugars and amino acids.[37] Compared with the number of reports on metal deposition on a carbon surface, there have been few results reported about uniform metal dispersion in carbon films such as McCreery et al.[57] Swain et al. recently reported a Pt/diamond composite film electrode fabricated with a three-step process: (i) continuous diamond thin-film deposition on a substrate, (ii) the electrodeposition of Pt particles on the diamond surface, and (iii) short-term diamond deposition to trap the Pt particles in the surface microstructure.[59]

In contrast, our group used the radio frequency (RF) method to form graphite-like carbon film containing highly dispersed nanoscale metal particles by co-sputtering metal and carbon. This method is simple. Various kinds of metal particles such as Pt, Ir, Cu, and Ni can be formed in carbon film at a relatively low sputtering temperature (<200 °C). Since the metal nanoparticles are tightly embedded in the film, the film is expected to be more stable than metal deposited carbon film. In addition, the flat surface of the film is better at suppressing background current.

3.2 Sputter-Deposited Carbon Film Electrode Containing Dispersed Pt and Ir Nanoparticles. Pt electrodes have been commonly used for detecting hydrogen peroxide, because a Pt electrode oxidizes hydrogen peroxide at around 500 mV vs Ag/AgCl. However, the Pt electrode surface is not stable during measurements. The background current varies gradually for several hours after the potential has been applied. This baseline shift poses a serious problem when we measure trace level biochemicals such as hormones and neurotransmitters.

Table 3. Metal-Nanoparticles and Carbon Film Composite Electrodes

Electrode material	Fabrication process	Measurement technique/Analyte	References
Nafion/Cu composite film on glassy carbon[a)]	Electrochemical deposition of Cu in Nafion	Carbohydrate detection by HPLC	33c
Cu modified on glassy carbon[a)]	Glassy carbon is immersed in $CuCl_2$ solution	Carbohydrate detection by HPLC	33b
Pt nanoparticles dispersed graphite like carbon film	Thermolysis of Pt doped poly(arylenediacetylene) at 600 °C	Characterization of film	38, 57
Pt incorporated mesoporous carbon	Mesoporous carbon obtained with mesoporous silicate template and Pt loaded from hexachloroplatinic acid	O_2 reduction	58
Pt or Ir dispersed graphite like carbon films	RF co-sputtered carbon and metal	Hydrogen peroxide detection Biosensor for glucose and glutamate HPLC for detecting acetylcholine	39, 63, 75
Ni or Cu dispersed graphite like carbon films	RF co-sputtered carbon and metal	Carbohydrate detection by HPLC	81, 82
Ni or Cu deposited boron doped diamond films	Electrochemical deposition of metal particles	Carbohydrate and amino acid by FIA	37
Pt and diamond composite film	Pt deposition on diamond film followed by short time diamond deposition	O_2 reduction	59

a) Electrode is not film electrode.

The detection limit of acetylcholine was improved by using an electrodeposited array of Pt particles on the gold film,[60] since a gold surface achieves a lower background current and Pt-microparticles work as microarray electrodes for hydrogen peroxide detection.

The combination of Pt particles and a carbon matrix achieves a better detection limit than Pt particles on gold films because the signal to noise ratio is improved if one disperses active nanoparticles in the carbon film. The sputtering procedure can easily control the Pt content to change the ratio of the Pt and carbon target areas. The film is more uniform than that prepared by electrochemical deposition since electrochemically deposited film has more particles near the electrode edge. In addition, the deposition charge must be precisely controlled since the particles often grow larger.

Figure 10A shows a transmission electron micrograph (TEM, front view) of Pt nanoparticle-dispersed carbon film.[39] The dark spots and light features correspond to the Pt nanoparticles and the carbon matrix, respectively. The lattice images of the carbon have a 3.6 Å spacing, which is wider than that of an ideal graphite crystal. This indicates that the carbon matrix is not amorphous, but is disordered graphite-like. Figure 10B shows a histogram of the Pt particle size distribution of the carbon film containing 2.9% Pt. The size of the Pt particles varies between 1 and 4 nm. Moreover, about 83% of the Pt particles fall in a narrow size range of 2 to 3 nm. The average diameter of the Pt particles is ~2.5 nm. This means that RF sputtering has the potential to be used as a method for preparing Pt particles with a narrow size distribution. The lattice spacing of the Pt-NEGCF measured by electron diffraction Pt(111) is 2.265 Å, which is in good agreement with the theoretical value for polycrystalline Pt. The lattice spacing measured with a side view image is similar to that measured with the front view. The average particle size obtained for two different Pt atom concentrations (1.3% and 6.5%) in the film is about 2.5 nm, the same as that for film containing 2.9% Pt. The variation in Pt content does not change the Pt

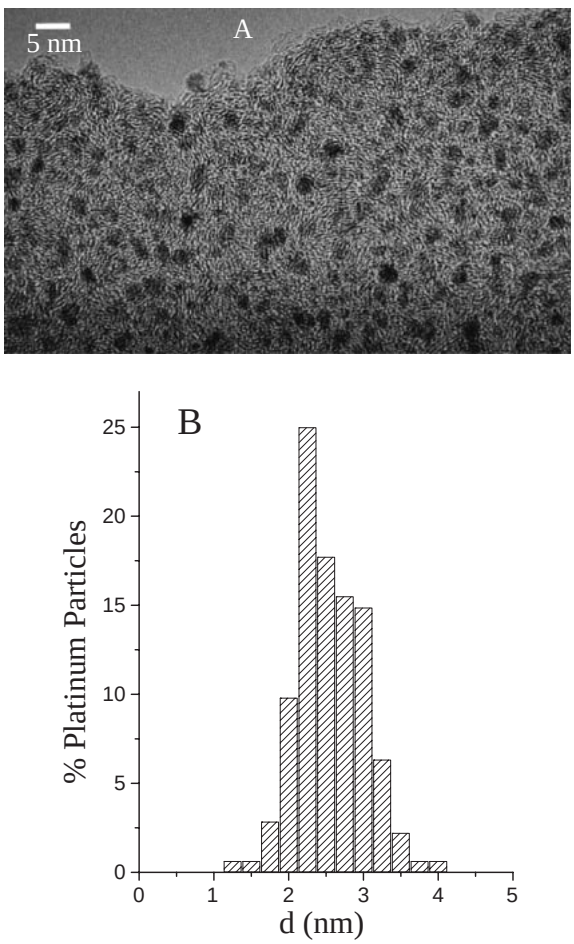

Fig. 10. Transmission electron micrograph (TEM) image (A) and histogram of the Pt size distribution (B) of the 2.9% Pt dispersed carbon film.[39]

nanoparticle size. McCreery et al. reported that the Pt particle size increases with higher Pt atom concentrations. They prepared 0.9%, 1.1%, and 1.5% Pt–GCs, with average cluster sizes of 8 Å, 10 Å, and 15 Å, respectively.[38,57] The RF sputtering method produces a different type of Pt nanoparticle dispersed carbon film from that prepared by the thermolysis of Pt complex polymer. XPS analysis shows that the Pt state in the carbon film is Pt(0). This binding energy (~1.0 eV) is slightly higher than that of bulk polycrystalline Pt. The difference may be due to the size effect of the small particles. The conductivity of RF carbon film is 24 $S \cdot cm^{-1}$, which is much higher than that of amorphous carbon film ($\sim 10^{-2}$ S/cm)[61] because the graphite-like structure was observed in the carbon film as shown in Fig. 10A. The conductivity of the Pt dispersed carbon film electrode increases from 24 to 103 $S \cdot cm^{-1}$ due to the highly dispersed Pt in the carbon. As reported for an electrochemically deposited Pt cluster on a carbon film used for studying fuel cell electrodes, the Pt nanoparticle-dispersed carbon film electrode exhibit high electrocatalytic activity for H^+ and dioxygen reduction when its current densities are compared with those at a bulk Pt electrode. The exchange current density increases as the Pt particle size decreases.[62] The interesting property of the film electrode when compared with a Pt bulk electrode is its stability. The current at the film electrode does not decay as quickly as that at a Pt-bulk electrode. The current density at the film electrode decreased 25% after 2 h of potential scanning, while it decreased about 80% at the Pt-bulk electrode. Moreover, the hydrogen evolution potential became positive as the Pt particle size decreased.

Electrodes for bio-electrochemical applications must be capable of the highly sensitive detection of hydrogen peroxide. Figure 11 shows hydrodynamic voltammograms (HDVs) of hydrogen peroxide for a film electrode containing 2.9% Pt in a thin layer radial flow cell, obtained by flow injection analysis (FIA). The current density at the GC electrode is very low, due to its high overpotential for hydrogen peroxide oxidation. In contrast, the electrocatalytic current density at the 2.9% Pt nanoparticle dispersed carbon film electrode was ten times higher than that obtained at the Pt-bulk electrode. The oxidation peak potential was ~0.57 V at the Pt nanoparticles-dispersed carbon film electrode, which is 70 mV lower than that

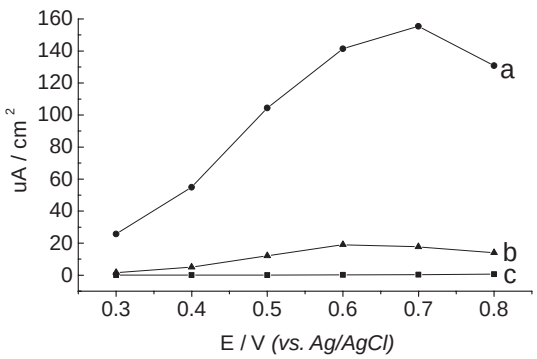

Fig. 11. Hydrodynamic voltammograms of 100 μM hydrogen peroxide at 2.9% Pt-nanoparticle dispersed carbon film electrode (a), Pt-bulk (b) and GC (c) electrodes. Sample injection, 20 μL; run buffer, 0.1 M PBS, pH 7; flow rate, 0.5 mL/min.[39]

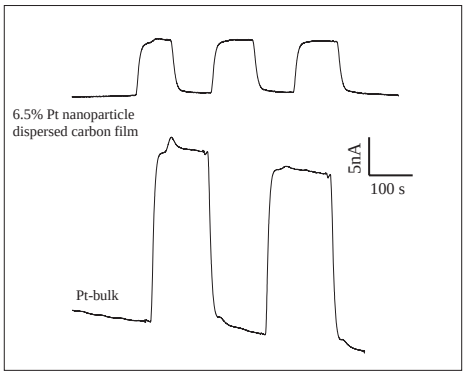

Fig. 12. Response of 10 μM glucose at GOx-modified 6.5% Pt-nanoparticles (A) and GOx-modified Pt bulk (B) electrodes. Detection potential 0.6 V vs Ag/AgCl; run buffer, 0.1 M PBS, pH 7; flow rate, 10 μL/min.[63]

at the Pt-bulk electrode. The lower oxidation potential and higher current density at the film electrode reveal its high electrocatalytic ability with regard to the electrooxidation of hydrogen peroxide.

The Pt nanoparticles-dispersed carbon film electrode is also very stable during measurements. Figure 12 shows the glucose response at both (A) the glucose oxidase-modified Pt nanoparticles-dispersed carbon film electrode (6.5% Pt content) and (B) glucose oxidase Pt-bulk electrode.[63] A stable baseline can be obtained at the Pt nanoparticles-dispersed carbon film electrode, while the baseline decreases quickly at the Pt bulk electrode. In addition, the baseline current of the 6.5% Pt nanoparticles-dispersed carbon film electrode is much lower than that of the Pt bulk electrode. This surface deactivation is particularly serious when the electrode is used to detect trace amounts of biochemicals such as neurotransmitters and hormones, because it takes a long time to obtain a stable baseline current. The performance of the Pt nanoparticles-dispersed carbon film electrode is examined by using the electrode to determine acetylcholine (ACh) and choline (Ch) separated by microbore liquid chromatography with a postcolumn enzyme reactor. Figure 13 shows chromatograms of 0.1 pmol ACh and Ch at both Pt bulk and Pt nanoparticles-dispersed carbon film electrodes. The currents for ACh and Ch obtained at the 6.5% Pt nanoparticles-dispersed carbon film electrode (0.382 and 0.448 nA) are lower than those obtained at the Pt bulk electrode (1.025 nA and 1.03 nA for ACh and Ch, respectively). However, the advantage of the Pt nanoparticles dispersed carbon film electrode is its small baseline drift and low noise level. In Fig. 13, the Pt bulk electrode shows a 2.154 nA baseline drift in 16 min. In contrast, the baseline changed only 0.006 nA (<0.003% of that at the Pt bulk electrode) at the 6.5% Pt nanoparticles-dispersed carbon film electrode. One reason for the stable behavior could be the stability of Pt nanoparticles against oxidation, as described in relation to the XPS result. In contrast, the Pt bulk electrode is more easily oxidized and becomes deactivated. A previous report[57b] also suggests that the carbon matrix in the film adsorbs the impurities, resulting in less deactivation of the Pt nanoparticle surface. As a result, the baseline noise at the Pt nanoparticles-dispersed carbon film electrode is lower than that of the Pt-bulk electrode; thus low detection limits of 2.5 and 2.3 fmol (S/N = 3) can be ob-

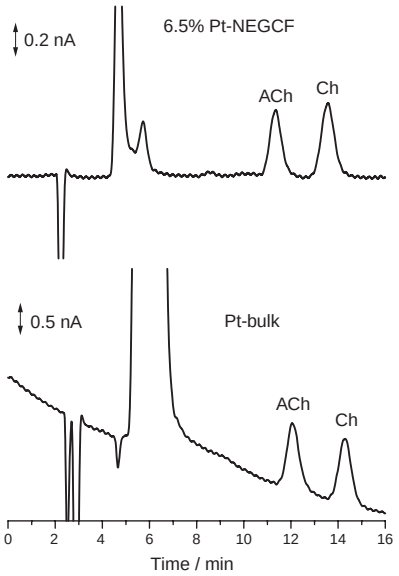

Fig. 13. Chromatograms of 0.1 pmol each of ACh and Ch at 6.5% Pt-nanoparticle dispersed carbon film electrode (A) and Pt bulk (B) electrodes, respectively. Detection potential, 0.6 V vs Ag/AgCl; buffer solution, 50 mM Na_2HPO_4 containing 0.5 mM EDTA at pH 8.0; flow rate, 120 μL/min.[63]

tained for ACh and Ch (Fig. 13). The detection limit is one order of magnitude higher for comparative experiments conducted at the Pt bulk electrode (23 fmol for ACh and 21 fmol for Ch). The detection limits are also lower than those in previous reports[64] using a Pt electrode. This indicates that the Pt nanoparticles-dispersed carbon film electrode is suitable for the highly sensitive measurement of biochemicals.

The co-sputtering process was also employed for preparing Ir nanoparticles-dispersed carbon film electrodes. Considerable interest has focused on Ir and Ir oxide (IrOx) electrodes due to their unique electrochemical properties, which include an excellent pH response,[65] and excellent electrocatalytic activity with regard to O_2 evolution,[66] Cl_2 evolution,[67] nitrite and nitrous oxide reduction,[68] insulin oxidation,[69] methanol oxidation,[70] and H_2 and O_2 reduction.[71] Rivas et al. have studied the performance of a glucose biosensor prepared by electrodepositing Ir with glucose oxidase (GOx) on carbon electrodes[72] and introducing Ir powder into carbon paste.[73] Ir incorporation can greatly improve both sensitivity and selectivity and also reduce the interference caused by ascorbic acid.[74] With the sputtering method, Ir particles, whose average size was 2 nm, were homogeneously dispersed in a carbon matrix. XPS revealed two chemical states of Ir (Ir(0) and Ir(IV)) in the film.[75] The film electrode exhibited excellent electrocatalytic ability with regard to H_2O_2 reduction, with a low atomic concentration compared to that of the bulk Ir electrode. The increase in the AA-induced peak was negligible at a detection potential of −0.15 V after a series of injections of 100 μM of hydrogen peroxide and hydrogen peroxide containing the same concentration of L-ascorbic acid (AA). The Ir nanoparticles-dispersed carbon film can be employed as an electrode for enzyme sensors such as that used for L-glutamic acid detection, which is operated at a low potential.

3.3 Carbon Film Electrodes with Dispersed Cu and Ni Nanoparticles. The electrochemical detection of sugars and carbohydrates was developed to achieve a low detection limit at a low cost. Two electrochemical detection techniques have been reported. One is the pulsed amperometric detection (PAD) method, which employs noble metals (Au, Pt) as working electrodes.[76] The PAD instrument is now commercially available and provides greater sensitivity than the optical method. However, PAD detection requires a regeneration step using the repetitive application of a pulsed potential waveform to renew the electrode surface because the surface of a noble metal electrode is easily fouled. The other method is constant potential amperometric detection with transition metal electrodes such as Cu and Ni.[33] With Cu and Ni electrodes, carbohydrates can be detected in alkaline media with the constant potential application method. However, a problem with constant potential amperometry is that there is a gradual reduction in the current response because of the loss of the electrode surface activity.[77] Several studies of Ni alloy electrodes[78] and Cu oxide with carbon powder composite electrodes[79] have been reported to improve both catalytic activity and stability. Kuwana et al.[78a] reported that Ni–Cr and Ni–Ti electrodes show improved sensitivity and good resistance to electrode surface fouling for carbohydrate detection. The deposition of Ni or Cu on commonly used electrodes such as carbon and diamond film has been reported.[80] The carbon film containing dispersed Ni or Cu nanoparticles shows excellent performance for detecting carbohydrate with good stability. The TEM images and narrow XPS spectra of Cu 2p for carbon film containing 4.5% and 2.6% Cu are shown in Fig. 14.[81] The Cu nanoparticles are 4–5 nm in size and are highly dispersed, similar to the Pt and Ir nanoparticles dispersed in carbon films (Fig. 10A). For the film with 4.5% Cu content, the main peak is at 934.4 eV, with a satellite line and shoulder peak at 932.8 eV. The satellite is attributed to the fact that the chemical state of Cu is a mixture of $Cu(OH)_2$ (934.4 eV) and Cu_2O (932.8 eV). The predominant component is not Cu_2O but $Cu(OH)_2$. In contrast, for the film with 2.6% Cu content, the main peak is 932.8 eV, suggesting that the Cu nanoparticles in the 2.6% film mainly consist of Cu_2O. The conductivity of the film increases with increasing Cu content similar to the carbon film with dispersed Pt nanoparticles. The conductivity of RF sputtered graphite-like carbon film is 24 S/cm. After co-sputtering Cu and carbon, the conductivity for 2.6% and 4.5% Cu nano-

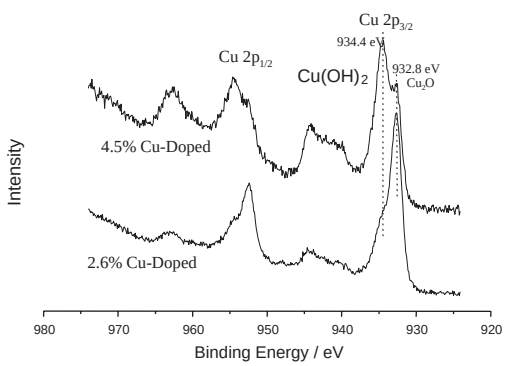

Fig. 14. Narrow XPS spectra of Cu 2p for 4.5% and 2.6% Cu-nanoparticles dispersed carbon film electrodes.[81]

particles-dispersed carbon film increases to 28.62 and 42.55 S/cm, respectively. The electrocatalytic ability of the film depends on the Cu state in the film. Figure 15 shows hydrodynamic voltammograms for the Cu nanoparticles-dispersed carbon film electrodes with 2.6% and 4.5% Cu content. The current for the detection of glucose at a Cu_2O-rich film electrode (2.6%) increases very slowly compared with that at a $Cu(OH)_2$-rich (4.5%) film electrode. At higher applied potentials (0.65 and 0.70 V), the current at the $Cu(OH)_2$-rich (4.5%) film electrode is more than 4 times higher than that at the Cu_2O-rich film electrode, while the ratio of the Cu concentrations in the two films is less than two. The higher state of Cu(III) (e.g., CuO(OH)) is supposed to participate in the electrooxidation process of glucose in an alkaline solution. The higher concentration of Cu(II) (e.g., $Cu(OH)_2$) may be more easily oxidized to CuO(OH) at the electrode surface.

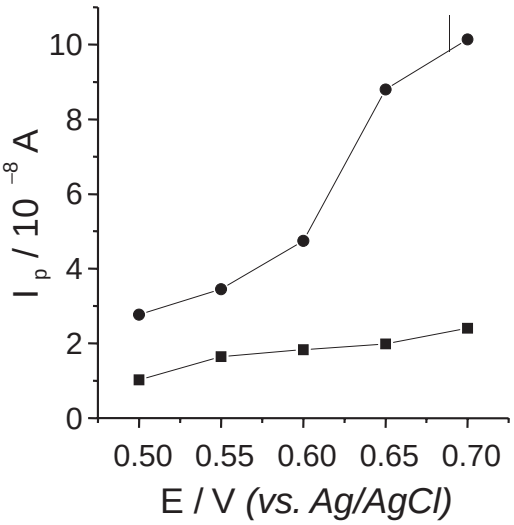

Fig. 15. Hydrodynamic voltammograms of 100 μM glucose at 4.5% (a) and 2.6% (b) Cu-nanoparticles dispersed carbon film electrodes. Sample injection, 20 μL; solution; 0.1 M NaOH, flow rate, 0.5 mL/min.[81]

Figure 16 shows high-resolution spectra of Ni nanoparticles dispersed carbon film electrodes. The Ni 2p spectrum shows the satellite line at a higher binding energy, in addition to the expected Ni $2p_{1/2}$ and Ni $2p_{3/2}$ lines. As regards the Ni $2p_{3/2}$ line, the peak around a binding energy of 853.0 eV is attributed to metallic Ni, while the peaks at higher energies (>855.0 eV) are associated with Ni hydroxide ($Ni(OH)_2$)/Ni oxide (NiO and Ni_2O_3).[82] The peaks around binding energies of 855.0, 855.6 and 855.8, 856.3 and 856.6 eV can be assigned to the Ni $2p_{3/2}$ photoelectrons from NiO, Ni_2O_3, NiO multiplet splitting, and $Ni(OH)_2$, respectively. The formation of oxide and hydroxide in the film is similar to that observed in Cu nanoparticles-dispersed carbon film electrode.[81] The Ni and Cu oxide and hydroxide formation are attributed to the effect of a very few water molecules adsorbed on the wall of the RF chamber, which is similar to the previously reported effect of water on the oxidation of a Ni surface in a vacuum.[83]

Excellent electrocatalytic properties for oxidizing carbohydrates can be achieved due to the above chemical structure of Ni nanoparticles in carbon film. Figure 17 shows cyclic voltammograms obtained in a 0.1 M NaOH solution (a) in the presence of 1 mM glucose (b) at the 0.8% Ni nanoparticles-

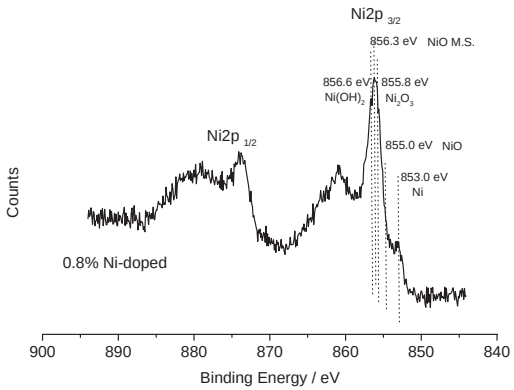

Fig. 16. High-resolution XPS spectrum of Ni 2p in 0.8% Ni-nanoprticles dispersed carbon film electrode.[82]

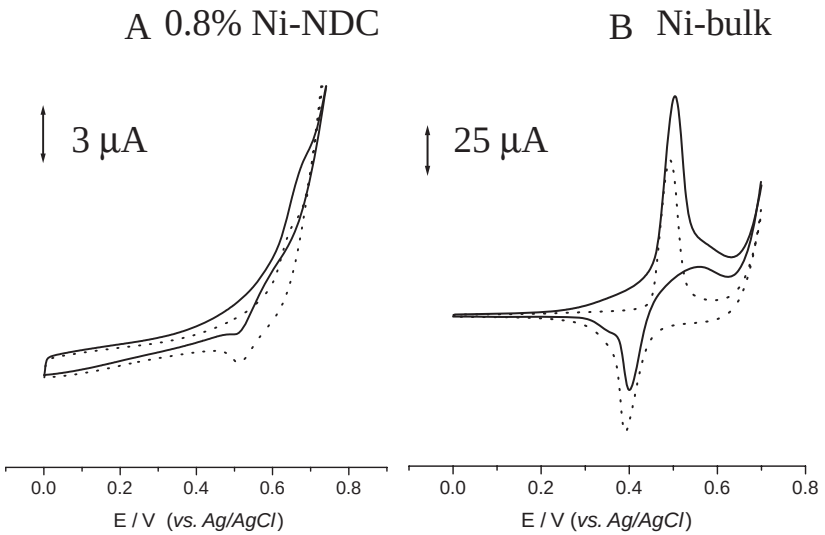

Fig. 17. Cyclic voltammograms in 0.1 M NaOH solution (a) and same solution containing 1 mM glucose (b) at 0.8% Ni-nanoparticles dispersed carbon film (A) and Ni-bulk (B) electrodes, respectively. Scan rate, 50 mV/s.[82]

dispersed carbon film (A) and Ni-bulk electrodes. The anodic and cathodic peaks in the 0.1 M NaOH solution (a) are assigned to the Ni(II)/Ni(III) redox couple, which is thought to catalyze the oxidation of small organic molecules. The background current of Ni nanoparticles-dispersed carbon film electrode is much lower than that of the bulk electrode because of the much lower Ni content. The peak currents for glucose (corrected for the background current of 0.1 M NaOH) are 3.5 and 35 μA at the 0.8% Ni nanoparticles dispersed carbon film and Ni-bulk electrodes, respectively. Considering the low Ni content (0.8%) and no electrocatalytic reaction of glucose at the pure carbon film, one can calculate the current density at the film electrode to be over 10 times that at the Ni-bulk electrode. The high current density and low background current are advantageous as regards improving the detection limit. The excellent electrocatalytic performance of the Ni nanoparticles-dispersed carbon film electrode was confirmed by hydrodynamic voltammograms (HDV) of glucose with the Ni nanoparticles-dispersed carbon film and Ni-bulk electrodes. With HDV, we also observed the same high current density of the film electrode as was observed with the CV measurement. The peak reaches its highest value at around 0.55 V for a Ni-bulk electrode. In contrast, the current response at the film electrode increases gradually when the applied potential is lower than 0.25 V and reaches its plateau above 0.4 V. This also suggests the excellent electrocatalytic property of the Ni nanoparticles in the carbon film. The excellent electrocatalytic performance also improves the stability. The CV measurement revealed no electrode fouling during 100 measurement cycles. With a flow injection analysis of 100 μM glucose after the baseline had been stabilized (only 30 min), the response at the film electrode decreased to 90% of its initial value and became stable after 2 h, whereas it decreased to 70% of its initial value at the Ni-bulk electrode. The performance of a Ni nanoparticles-dispersed carbon film electrode can be evaluated in combination with HPLC. Figure 18A shows a chromatogram of 10 μM each of glucose, fructose, sucrose, and lactose detected at the 0.8% Ni nanoparticles-dispersed carbon film electrode, following separation by a anion exchange column at an applied potential of 0.40 V. The peaks of four sugars can be clearly observed in the figure. In contrast, the response of the sugars at the Ni-bulk electrode was very low under the same conditions (Fig. 18B), indicating that the film electrode shows high sensitivity and a low detection limit with a lower applied potential. Figure 18C shows a chromatogram of a solution of 0.05 μM mixed sugars. The detection limits (LODs, $S/N = 3$) calculated from Fig. 18C are 20, 25, 50, and 37 nM (or 0.2, 0.25, 0.5, and 0.37 pmol) for glucose, fructose, sucrose, and lactose, respectively. These values are lower than those obtained at a Ni-bulk electrode (4 pmol, for glucose)[77] and Ni alloy (between 0.5 and 1 pmol)[78b] and Ni-based CME (between 3.3 and 5.5 pmol)[84] electrodes under optimized detection conditions (0.55 or 0.6 V vs Ag/AgCl). The reproducibility of 10 cycle HPLC detection showed a variation of less than 5.0% for each sugar with the film electrode.

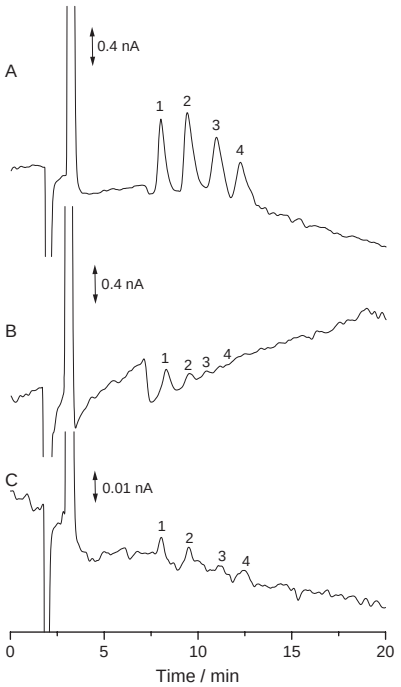

Fig. 18. Liquid chromatogram separation of mixture of glucose (1), fructose (2), sucrose (3), and lactose (4) at 0.8% Ni-nanoparticles dispersed carbon film electrode (A, C) and Ni-bulk (B) electrodes carried out with 0.03 M NaOH as mobile phase. Separation column, Hamilton RCX-10 anion exchange column (250 × 4 mm^2 i.d.) plus carboPac PA 100 guard column (50 × 4 mm^2 i.d.); injection volume, 10 μL, Concentration of sugars, 10 μM (A, B), 0.05 μM (C), flow rate, 1.0 mL/min, applied potential, 0.40 V vs Ag/AgCl.

4. Conclusion and Future Trend

This paper has reviewed the recent development of electroanalysis using carbon film electrodes, microfabricated carbon film electrodes, and carbon film electrodes containing dispersed metal nanoparticles. Carbon films are important since they have a wider potential window and a low background current compared with metal films. The ECR sputter-deposited carbon shows a wider potential window and high stability, since it has a very flat surface and is less adsorptive as regards electrochemically oxidized products such as alkylphenols. Carbon films can be fabricated into microarray electrodes with various shapes using a new fabrication process. Carbon-based IDA electrodes achieve a low detection limit and are suitable for use as highly sensitive electrodes for LC and CE. Individually addressable split-disk or 8 × 8 microarray electrodes are fabricated for multi-potential detection and electrochemical real-time imaging, respectively. The carbon film based dual electrode is modified with enzyme and mediator, integrated in a microfluidic channel and used for the continuous measurement of L-glutamate released from cultured cells.

Carbon films containing dispersed metal nanoparticles are prepared by co-sputtering metal and carbon. Various metal nanoparticles such as Pt, Ir, Cu, and Ni can be dispersed in the carbon films. Excellent electrocatalytic performance and a stable surface are obtained with the carbon film containing Pt. A low detection limit for ACh and Ch is obtained when the electrode is used as the detection electrode in liquid chromatography. In contrast, Cu or Ni dispersed-carbon film electrodes exhibit high electrocatalytic activity for sugars in alka-

line media due to the metal hydroxide structure in the nanoparticles. Improved detection limits for sugars are also obtained using carbon films with dispersed Ni nanoparticles.

Carbon film-based electrodes will become more important because the recent development of new carbon materials such as diamond films and carbon nanotubes has extended the application area of electroanalysis. Carbon film with a mesoporous structure will be useful for achieving high selectivity, since selective molecular recognition with mesopores and the incorporation of metals allows us to achieve excellent electrocatalytic performance with a large surface area. The micro and nanofabrication of the above carbon films should be developed and employed for various analytical devices, such as on-chip LC, CE, and various sensing devices.

The author thanks the following people who worked together on the present study: Dr. Masao Morita, Dr. Tsutomu Horiuchi, Dr. Masaya Takahashi, Dr. Yuzuru Iwasaki, Dr. Keiichi Torimitsu, Dr. Yuko Ueno, Dr. Nahoko Kasai, Dr. Tianyan You, Dr. Zhiming Liu, Katsuyoshi Hayashi and Wakako Tanaka at NTT corporation, Hisao Tabei, Dr. Makoto Hikita at NTT-AT corporation, Dr. Ryoji Kurita at AIST, Prof. Koichi Aoki at Fukui University, Prof. Kazutaka Maeyama and Dr. Shoko Iwaki at Ehime University, Prof. Katsuyuki Tanizawa at Osaka University, Prof. Takeshi Kato at Yokohama City University, Prof. Koji Suzuki and his group at Keio University, Prof. W. R. Heineman and his group at University of Cincinnati, Dr. Shigeru Hirono at NTT-Afty Corporation, Dr. Toshiaki Tamamura at Nano-F corporation, Dr. Masato Tomita at Corning Japan and Katsunobu Yamamoto at BAS corporation and Dr. P. T. Kissinger and his co-workers at Bioanalytical Systems Inc.

References

1 P. T. Kissinger and W. R. Heineman, "Laboratory Techniques in Electroanalytical Chemistry," 2nd ed, Marcel Dekker, NY (1996).

2 M. Fleischman, S. Pons, D. Rolison, and P. P Schmidt, "Ultramicroelectrodes," Datatech Science, Morganton, NC (1987).

3 R. M. Wightman, *Anal. Chem.*, **53**, 1125A (1981).

4 E. L. Ciolkowski, B. R. Cooper, J. A. Jankowski, J. W. Jorgenson, and R. M. Wightman, *J. Am. Chem. Soc.*, **114**, 2815 (1992).

5 R. T. Kennedy, L. Huang, M. A. Atkinson, and P. Dush, *Anal. Chem.*, **65**, 1882 (1993).

6 a) K. T. Kawagoe, P. A. Garris, and R. M. Wightman, *J. Electroanal. Chem.*, **359**, 193 (1993). b) K. Pihel, Q. D. Walker, and R. M. Wightman, *Anal. Chem.*, **68**, 2084 (1996).

7 a) H. S. White, G. P. Kittlesen, and M. S. Wrighton, *J. Am. Chem. Soc.*, **106**, 5375 (1984). b) G. P. Kittlesen, H. S. White, and M. S. Wrighton, *J. Am. Chem. Soc.*, **106**, 7389 (1984).

8 A. J. Bard, J. A. Crayston, G. P. Kittlesen, T. V. Shea, and M. S. Wrighton, *Anal. Chem.*, **58**, 2321 (1986).

9 a) O. Niwa and T. Tamamura, *J. Chem. Soc., Chem. Commun.*, **1984**, 817. b) M. Hikita, O. Niwa, A. Sugita, and T. Tamamura, *Jpn. J. Appl. Phys.*, **24**, L79 (1985). c) O. Niwa, M. Hikita, and T. Tamamura, *Synth. Met.*, **18**, 677 (1987).

10 a) K. Aoki, M. Morita, O. Niwa, and H. Tabei, *J. Electroanal. Chem.*, **256**, 269 (1988). b) O. Niwa, M. Morita, and H. Tabei, *Anal. Chem.*, **62**, 447 (1990). c) T. Horiuchi, O. Niwa, M. Morita, and H. Tabei, *J. Electroanal. Chem.*, **295**, 25 (1990).

11 A. Aoki, T. Matsue, and I. Uchida, *Anal. Chem.*, **62**, 2206 (1990).

12 a) A. L. Beilby and A. Carlsson, *J. Electroanal. Chem.*, **248**, 283 (1988). b) C. F. McFadden, L. L. Russell, P. R. Melaragno, and J. A. Davis, *Anal. Chem.*, **62**, 742 (1990). c) J. K. Clark, W. A. Schilling, C. A. Wijayawardhana, and P. R. Melaragno, *Anal. Chem.*, **66**, 3528 (1994). d) T.-Y. Kim, D. M. Scarnulis, and A. G. Ewing, *Anal. Chem.*, **58**, 1782 (1986). e) K. Lundstrom, *Anal. Chim. Acta*, **146**, 97 (1983). f) K. Lundstrom, *Anal. Chim. Acta*, **146**, 109 (1983).

13 A. Rojo, A. Rosenstratten, and D. Anjo, *Anal. Chem.*, **58**, 2988 (1986).

14 H. Tabei, M. Morita, T. Horiuchi, and O. Niwa, *J. Electroanal. Chem.*, **334**, 25 (1992).

15 O. Niwa and H. Tabei, *Anal. Chem.*, **66**, 285 (1994).

16 R. Schlesinger, M. Burns, and H.-J. Ache, *J. Electrochem. Soc.*, **144**, 6 (1997).

17 a) G. C. Fiaccabrino, X.-M. Tang, N. Skinner, N. F. De Rooij, and M. Koudelka-Hep, *Sens. Actuators, B*, **35–36**, 247 (1996). b) G. C. Fiaccabrino, X.-M. Tang, N. Skinner, N. F. De Rooij, and M. Koudelka-Hep, *Anal. Chim. Acta*, **326**, 155 (1996).

18 a) J. Kim, X. Song, K. Kinoshita, M. Madou, and R. White, *J. Electrochem. Soc.*, **145**, 2315 (1998). b) A. M. Lyons, L. P. Hale, and C. W. Wilkins, *J. Vac. Sci. Technol., B*, **3**, 447 (1985).

19 a) H. Tabei, O. Niwa, T. Horiuchi, and M. Morita, *Denki Kagaku*, **61**, 820 (1993). b) O. Niwa, T. Horiuchi, and H. Tabei, *J. Electroanal. Chem.*, **367**, 265 (1994).

20 a) J. Wang, Q. Chen, C. L. Renschler, and C. White, *Anal. Chem.*, **66**, 1988 (1994). b) J. Wang, A. Brennsteiner, A. P. Sylwester, and C. L. Renschler, *Electroanalysis*, **3**, 505 (1991). c) C. L. Renschler, A. P. Sylwester, and L. V. Salgado, *J. Mater. Res.*, **4**, 452 (1989).

21 J. Xu, M. C. Granger, Q. Chen, J. M. Strojek, T. E. Lister, and G. M. Swain, *Anal. Chem.*, **69**, 591A (1997).

22 T. N. Rao and A. Fujishima, *Diamond Relat. Mater.*, **9**, 384 (2000).

23 R. G. Compton, J. S. Foord, and F. Marken, *Electroanalysis*, **15**, 1349 (2003).

24 J. J. Blackstock, A. A. Rostami, A. M. Nowak, R. L. McCreery, M. R. Freeman, and M. T. McDernott, *Anal. Chem.*, **76**, 2544 (2004).

25 T. You, O. Niwa, M. Tomita, T. Ichino, and S. Hirono, *J. Electrochem. Soc.*, **149**, E479 (2002).

26 a) O. Niwa, M. Morita, B. P. Solomon, and P. T. Kissinger, *Electroanalysis*, **8**, 427 (1996). b) O. Niwa and M. Morita, *Anal. Chem.*, **68**, 355 (1996). c) Y. Iwasaki, O. Niwa, M. Morita, H. Tabei, and P. T. Kissinger, *Anal. Chem.*, **68**, 3797 (1996). d) Z. Liu, O. Niwa, R. Kurita, and T. Horiuchi, *Anal. Chem.*, **72**, 1315 (2000).

27 a) O. Niwa, H. Tabei, B. P. Solomon, F. Xie, and P. T. Kissinger, *J. Chromatogr., B*, **670**, 21 (1995). b) Z. Liu, O. Niwa, R. Kurita, and T. Horiuchi, *J. Chromatogr., A*, **891**, 149 (2000).

28 A. T. Woolley, K. Q. Lao, A. N. Glazer, and R. A. Mathies, *Anal. Chem.*, **70**, 684 (1998).

29 R. P. Baldwin, T. J. Roussel, M. M. Crain, V. Bathlagunda, D. J. Jackson, J. Gullapalli, J. A. Conklin, R. Pai, J. F. Naber, K. M. Walsh, and R. S. Keynton, *Anal. Chem.*, **74**, 3690 (2002).

30 a) O. Niwa, T. Horiuchi, R. Kurita, H. Tabei, and K. Torimitsu, *Anal. Sci.*, **14**, 947 (1998). b) O. Niwa, R. Kurita, T. Horiuchi, and K. Torimitsu, *Electroanalysis*, **11**, 356 (1999).

31 R. Kurita, K. Hayashi, X. Fan, K. Yamamoto, T. Kato, and O. Niwa, *Sens. Actuators, B*, **87**, 296 (2002).

32 a) O. Niwa, R. Kurita, Z. Liu, T. Horiuchi, and K. Torimitsu, *Anal. Chem.*, **72**, 949 (2000). b) O. Niwa, R. Kurita, K. Hayashi, T. Horiuchi, K. Torimitsu, K. Maeyama, and K. Tanizawa, *Sens. Actuators, B*, **67**, 43 (2000). c) S. Iwaki, M. Ogasawara, R. Kurita, O. Niwa, K. Tanizawa, Y. Ohashi, and K. Maeyama, *Anal. Biochem.*, **304**, 236 (2002). d) R. Kurita, K. Hayashi, K. Torimitsu, and O. Niwa, *Anal. Sci.*, **19**, 1581 (2003).

33 a) J. B. Kafil and C. O. Huber, *Anal. Chim. Acta*, **175**, 275 (1985). b) L. M. Santos and R. P. Baldwin, *Anal. Chem.*, **59**, 1766 (1987). c) J. M. Zadeii, J. Marioli, and T. Kuwana, *Anal. Chem.*, **63**, 649 (1991).

34 a) S. C. Davis and K. J. Klabunde, *Chem. Rev.*, **82**, 153 (1982). b) B. X. Wang and X. Y. Li, *Anal. Chem.*, **70**, 2181 (1998). c) A. A. Mikhaylova, O. A. Khazova, and V. S. Bagotzky, *J. Electroanal. Chem.*, **480**, 225 (2000).

35 a) I. G. Casella and M. Contursi, *Anal. Chim. Acta*, **478**, 179 (2003). b) I. G. Casella and M. Contursi, *Anal. Bioanal. Chem.*, **376**, 673 (2003).

36 J. M. Zadeii, J. Marioli, and T. Kuwana, *Anal. Chem.*, **63**, 649 (1991).

37 R. Uchikado, T. N. Rao, D. A. Tryk, and A. Fujishima, *Chem. Lett.*, **2001**, 144.

38 N. L. Pocard, D. C. Alsmeyer, R. L. McCreery, T. X. Neenan, and M. R. Callstrom, *J. Am. Chem. Soc.*, **114**, 769 (1992).

39 T. You, O. Niwa, T. Horiuchi, M. Tomita, Y. Iwasaki, Y. Ueno, and S. Hirono, *Chem. Mater.*, **14**, 4796 (2002).

40 a) M. D. Koppang, M. Witek, J. Blau, and G. M. Swain, *Anal. Chem.*, **71**, 1188 (1999). b) J. Xu and G. M. Swain, *Anal. Chem.*, **70**, 1502 (1998).

41 a) C. Terashima, T. N. Rao, B. V. Sarada, D. A Tryk, and A. Fujishima, *Anal. Chem.*, **74**, 895 (2002). b) N. Spataru, B. V. Sarada, E. Popa, D. A. Tryk, and A. Fujishima, *Anal. Chem.*, **73**, 514 (2001). c) B. V. Sarada, T. N. Rao, D. A. Tryk, and A. Fujishima, *Anal. Chem.*, **72**, 1632 (2000).

42 A. Zeng, E. Liu, P. Hing, S. Zhang, S. N. Tan, I. F. Annergren, and J. Gao, *Int. J. Mod. Phys. B*, **16**, 1024 (2002).

43 A. Zeng, E. Liu, S. N. Tan, S. Zhang, and J. Gao, *Electroanalysis*, **14**, 1110 (2002).

44 J. Diaz, G. Paolicelli, S. Ferrer, and F. Comin, *Phys. Rev. B*, **54**, 8064 (1995).

45 S. Hirono, S. Umemura, M. Tomita, and R. Kaneko, *Appl. Phys. Lett.*, **80**, 425 (2001).

46 J. Robertson, *Adv. Phys.*, **35**, 317 (1986).

47 S. Jobling and J. P. Sumpter, *Aquat. Toxicol.*, **27**, 361 (1993).

48 A. Tanaka, H. Ban, and S. Imamura, *J. Vac. Sci. Technol., B*, **7**, 572 (1989).

49 S. Ranganathan, R. McCreery, S. M. Majii, and M. Madou, *J. Electrochem. Soc.*, **147**, 277 (2000).

50 K. Tsunozaki, Y. Einaga, T. N. Rao, and A. Fujishima, *Chem. Lett.*, **2002**, 502.

51 R. A. Wallingfors and A. G. Ewing, *Anal. Chem.*, **60**, 258 (1988).

52 K. Hayashi, Y. Iwasaki, R. Kurita, K. Sunagawa, and O. Niwa, *Electrochem. Commun.*, **5**, 1037 (2003).

53 a) H. Y. Liu, F. R. F. Fan, C. W. Lin, and A. J. Bard, *J. Am. Chem. Soc.*, **108**, 3838 (1986). b) T. Yasukawa, T. Kaya, and T. Matsue, *Anal. Chem.*, **71**, 4637 (1999).

54 a) N. Kasai, Y. Jimbo, O. Niwa, T. Matsue, and K. Torimitsu, *Neurosci. Lett.*, **304**, 112 (2001). b) K. Hayashi, T. Horiuchi, R. Kurita, K. Torimitsu, and O. Niwa, *Biosens. Bioelectron.*, **15**, 523 (2000).

55 J. H. Pei, M. L. Tercier-Waeber, J. Buffle, G. C. Fiaccabrino, and M. Koudelka-Hep, *Anal. Chem.*, **73**, 2273 (2001).

56 a) R. Kurita, H. Tabei, K. Hayashi, T. Horiuchi, K. Torimitsu, and O. Niwa, *Anal. Chim. Acta*, **441**, 165 (2001). b) R. Kurita, K. Hayashi, T. Horiuchi, O. Niwa, K. Maeyama, and K. Tanizawa, *Lab Chip*, **2**, 34 (2002).

57 a) M. R. Callstrom, T. X. Neenan, R. L. McCreery, and D. C. Alsmeyer, *J. Am. Chem. Soc.*, **112**, 4954 (1990). b) N. L. Pocard, D. C. Alsmeyer, R. L. McCreery, T. X. Neenan, and M. R. Callstrom, *J. Mater. Chem.*, **2**, 771 (1992). c) H. D. Howard, N. L. Pocard, D. C. Alsmeyer, O. J. A. Schueller, R. J. Spontak, M. E. Huston, W. Huang, R. L. McCreery, T. X. Neenan, and M. R. Callstrom, *Chem. Mater.*, **5**, 1727 (1993). d) O. J. A. Schueller, N. L. Pocard, M. E. Huston, R. J. Spontak, T. X. Neenan, and M. R. Callstrom, *Chem. Mater.*, **5**, 11 (1993).

58 S. H. Joo, S. J. Chol, I. Oh, J. Kwak, Z. Liu, O. Terasaki, and R. Ryoo, *Nature*, **412**, 169 (2001).

59 J. Wang and G. M. Swain, *J. Electrochem. Soc.*, **150**, E24 (2003).

60 O. Niwa, T. Horiuchi, M. Morita, T. Huang, and P. T. Kissinger, *Anal. Chim. Acta*, **318**, 167 (1996).

61 J. Robertson, *Adv. Phys.*, **35**, 317 (1986).

62 I. G. Casella and M. Contursi, *Anal. Chim. Acta*, **478**, 179 (2003).

63 T. You, O. Niwa, M. Tomita, and S. Hirono, *Anal. Chem.*, **75**, 2080 (2003).

64 a) F. Flentge, K. Venema, T. Koch, and J. Korf, *Anal. Biochem.*, **204**, 305 (1992). b) G. Damsma, B. H. C. Westerink, and A. S. Horn, *J. Neurochem.*, **45**, 1649 (1985).

65 a) T. Katsube, I. Lauks, and J. N. Zemel, *Sens. Actuators*, **2**, 399 (1982). b) L. D. Burke, J. K. Mulcahy, and D. P. Whelan, *J. Electroanal. Chem.*, **163**, 117 (1984).

66 S. Gottesfeld and S. Srinivasan, *J. Electroanal. Chem.*, **86**, 89 (1978).

67 a) D. N. Buckley and L. D. Burke, *J. Chem. Soc., Faraday Trans. 1*, **72**, 2431 (1976). b) J. Mozota and B. E. Conway, *J. Electrochem. Soc.*, **128**, 2141 (1981).

68 a) D. De, J. D. Englehardt, and E. E. Kalu, *J. Electrochem. Soc.*, **147**, 4224 (2000). b) R. Gomez and M. J. Weaver, *Langmuir*, **14**, 2525 (1998).

69 M. Pikulski and W. Gorski, *Anal. Chem.*, **72**, 2696 (2000).

70 R. Ortiz, O. P. Marquez, J. Marquez, and C. Gutierrez, *J. Phys. Chem.*, **100**, 8389 (2000).

71 a) M. C. Rodriguesz and G. A. Rovas, *Anal. Lett.*, **34**, 1829 (2001). b) S. A. Miscoria, G. D. Barrera, and G. A. Rovas, *Electroanalysis*, **14**, 981 (2002).

72 a) J. Wang, G. Rivas, and M. Chicharro, *J. Electroanal. Chem.*, **439**, 55 (1997). b) M. C. Rodríguez and G. Rivas, *Electroanalysis*, **11**, 558 (1999).

73 J. Wang, G. Rivas, and M. Chicharro, *Electroanalysis*, **8**, 149 (1996).

74 S. A. Miscoria, G. D. Barrera, and G. A. Rovas, *Electroanalysis*, **14**, 981 (2002).

75 T. You, O. Niwa, R. Kurita, Y. Iwasaki, K. Hayashi, K. Suzuki, and S. Hirono, *Electroanalysis*, **16**, 54 (2004).

76 a) D. C. Johnson and W. R. LaCourse, *Anal. Chem.*, **62**, 589A (1990). b) W. R. LaCourse and D. C. Johnson, *Carbohydr. Res.*, **251**, 159 (1991).

77 P. Luo, F. Zhang, and R. P. Baldwin, *Anal. Chim. Acta*,

244, 169 (1991).

78 a) J. Marioli, P. F. Luo, and T. Kuwana, *Anal. Chim. Acta*, **282**, 571 (1993). b) P. F. Luo and T. Kuwana, *Anal. Chem.*, **66**, 2775 (1994). c) M. Morita, O. Niwa, S. Tou, and N. Watanabe, *J. Chromatogr., A*, **837**, 17 (1999).

79 a) Y. Xie and C. O. Huber, *Anal. Chem.*, **63**, 1714 (1991). b) T. Ueda, R. Mitchell, F. Kitamura, and J. Nakamoto, *J. Chromatgr.*, **592**, 229 (1990).

80 a) S. V. Prabhu and R. P. Baldwin, *Anal. Chem.*, **61**, 852 (1989). b) K. Ohnishi, Y. Einaga, H. Notsu, C. Terashima, T. N. Rao, S. Park, and A. Fujishima, *Electrochem. Solid-State Lett.*, **5**, D1 (2002).

81 T. You, O. Niwa, M. Tomita, H. Ando, M. Suzuki, and S. Hirono, *Electrochem. Commun.*, **4**, 468 (2002).

82 T. You, O. Niwa, Z. Chen, K. Hayashi, M. Tomita, and S. Hirono, *Anal. Chem.*, **75**, 5191 (2003).

83 J. C. d Jesus, J. Carrazza, P. Pereira, and F. Zaera, *Surf. Sci.*, **369**, 217 (1996).

84 I. G. Casella and M. Gutta, *Electroanalysis*, **13**, 549 (2001).

Osamu Niwa was born in 1958 in Tsukumi-city in Oita Prefecture, Japan. He received his B. Eng. degree in 1981, M. Eng. in 1983, and Dr. Eng. in 1990 all from Kyushu University. He joined Nippon Telegraph and Telephone Public Corporation (Now, NTT Corporation) in 1983, and worked at NTT Ibaraki Labs. (1983–1987), NTT Basic Research Labs. (1987–1999), NTT Lifestyle and Environmental Technology Labs. (1999–2002), and NTT Microsystem Integration Labs. (2002–2004). He was also a visiting scholar in Prof. William R. Heineman's group in the Department of Chemistry at the University of Cincinnati (1990–1991). Since 2004, he has been the leader of the Biosensing Technology Research Group of the National Institute of Advanced Industrial Science and Technology (Tsukuba). His research is related to microfabricated electrodes including metal and carbon films and their application for detecting biochemicals, surface plasmon resonance measurement combined with electrochemistry, and microfluidic devices for detecting environmental pollutants.